ISTITUTO NAZIONALE DI FISICA NUCLEARE
Laboratori Nazionali di Frascati

LNF-85/36

A. Balerna, E. Bernieri, P. Picozzi, A. Reale, S. Santucci,
E. Burattini, S. Mobilio:

A STRUCTURAL INVESTIGATION ON SMALL GOLD CLUSTERS BY EXAFS

Estratto da:
Surface Sci. 156, p. 206 (1985)

Servizio Documentazione
dei Laboratori Nazionali di Frascati
Cas. Postale 13 - Frascati (Roma)

Surface Science 156 (1985) 206–213
North-Holland, Amsterdam

85/36

A STRUCTURAL INVESTIGATION ON SMALL GOLD CLUSTERS BY EXAFS

A. BALERNA, E. BERNIERI, P. PICOZZI, A. REALE and S. SANTUCCI
Istituto di Fisica, Universita' dell'Aquila, L'Aquila, Italy

and

E. BURATTINI and S. MOBILIO
INFN, Laboratori Nazionali Frascati, I-00044 Frascati, Italy

Received 13 July 1984; accepted for publication 24 September 1984

A structural investigation using extended X-ray absorption fine structure (EXAFS) spectra, recorded on Au metal clusters whose average dimension ranges from 11 to 50 Å, is reported. Data analysis performed on the first and second coordination shells, showed the presence of interatomic distance contractions, a lowering of the mean coordination number and an increasing EXAFS Debye–Waller factor at decreasing mean diameter of the clusters. No structural changes to icosahedra have been observed.

1. Introduction

Great importance has been given in the last years to the structural and electronic properties of small metal clusters, either for their physical peculiarities [1–5] or for their technological applications like heterogeneous catalysis [6].

The aim of this work is an investigation on the changes in structural properties of Au metal clusters, evaporated on a weakly interacting polymer substrate such as mylar.

Many experimental studies have been done in the past, using diffraction [7–9], but this technique shows two principal limits:

(1) it becomes less sensitive as the cluster size decreases and this gives a great disagreement between numerical values obtained on clusters of the same diameter [7–9];

(2) with this technique, the determination of lattice parameters is strictly related to Miller indices. A structural change from fcc to icosahedra, which is predicted for small metal clusters, can be wrongly interpreted as being due to contraction of the lattice parameter, if one uses Miller indices relative to an fcc structure [10].

In order to determine the effective amount of contractions and to check also changes in the cluster crystallographic structure [11,12], we did our structural investigation using a model-independent technique such as EXAFS (extended X-ray absorption fine structure).

2. Samples

Samples were prepared in vacuum, by evaporating on a 6 μm mylar film multiple layers of gold and mylar until the optimum metal thickness for X-ray measurements was achieved [13]. The amount of gold deposited on each layer of the different samples studied, is reported in table 1; mylar thickness was always around 200 Å. Gold and mylar depositions were both controlled with a quartz-crystal detector.

Discontinuity of the multilayer samples has been controlled with optical transmission measurements made at normal incidence in the spectral range 0.25–2.5 μm. In fact, transmittance spectra of discontinuous films, contrary to continuous ones, generally show a wide minimum below the interband transitions [14] due to the free electron in the metal particles and an high transmission in the near IR [15]. Comparisons between the optical transmission spectra of some samples and of continuous films demonstrated their discontinuity.

Cluster size distributions have been obtained using electron microscopy analysis (table 1).

3. Measurement of X-ray absorption spectra

The X-ray spectra, shown in fig. 1, have been recorded on the Au L_3 absorption edge both at liquid nitrogen temperature (LNT) and at room temperature (RT). Measurements have been done at the Frascati National

Table 1
Values of the coverages (t), mean diameters (D), and standard deviations (σ) of the diameters of the samples studied

t (atoms/cm^2)	D (Å)	σ (Å)
0.6×10^{15}	11.0	6.5
1.8×10^{15}	15.0	5.4
3.0×10^{15}	20.0	7.5
4.1×10^{15}	24.0	8.2
5.9×10^{15}	30.0	8.9
12.0×10^{15}	42.5	11.0
18.0×10^{15}	60.0	18.0

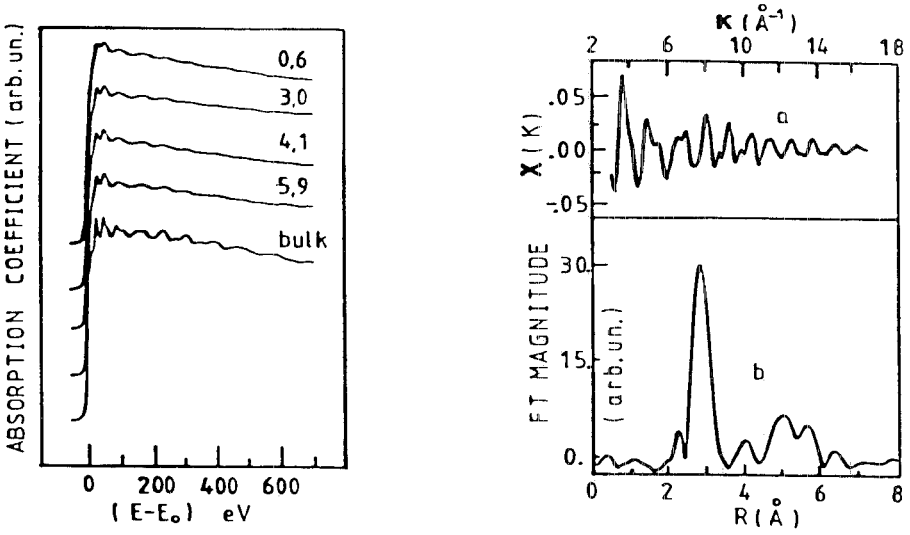

Fig. 1. X-ray absorption spectra recorded on the Au L_3 edge at 77 K. Coverages indicated in the figure are in units of 10^{15} atoms/cm^2. Energy zero has been assumed at the edge inflection point.

Fig. 2. (a) EXAFS spectrum of Au bulk at LNT and (b) Fourier transform in the k range 3–16 Å^{-1} using a gaussian window and a k^3 weight.

Syncrotron Radiation Laboratory using the wiggler photon beam line, with typically $I = 40$ mA and $E = 1.5$ GeV in the storage ring ADONE. The X-ray line monochromator was equipped with a Si(111) channel-cut crystal and the detection of the X-ray beam was achieved by two ionization chambers filled with Kr gas [16,17].

4. Analysis of X-ray absorption spectra

An EXAFS spectrum arises from the oscillations in the photoelectron cross section due to the scattering of the ejected photoelectron by atoms surrounding the absorbing atom. In order to extract this part from the X-ray absorption spectra, a standard procedure has been used [18]. The absorption coefficient is identified as:

$$\mu x = \ln(I_0/I),$$

where μ is the linear absorption coefficient, x is the sample thickness, I_0 is the incident X-ray intensity and I is the transmitted intensity. EXAFS of $\chi(k)$ is given by:

$$\chi(k) = [\mu(k) - \mu_0(k)]/\mu_0(k), \tag{1}$$

where μ_0 is the atomic absorption coefficient. It has been demonstrated [13] that relation (1), under the assumption of a single scattering process, can be formulated as:

$$\chi(k) = \sum_j S_0^2 N_j |f_j(k, \pi)| \frac{\exp(-2k^2\sigma_j^2)}{kR_j^2} \sin(2kR_j + \Phi_j), \tag{2}$$

where the index j indicates the jth neighbour shell of atoms surrounding the absorbing atom. N_j is the number of atoms in the jth shell, R_j is the distance from the absorbing atom and k is the photoelectron wave vector. σ_j is a correlated Debye–Waller factor, S_0^2 is a reduction due to multielectron excitation, $|f_j(k, \pi)|$ is the backscattering amplitude of the atoms in the jth shell and Φ_j is the electron phase shift that has a contribution from both the absorbing and the backscattering atoms.

As can be seen from relation (2), a $\chi(k)$ Fourier transform will give several peaks. The peaks positions correspond to the different coordination shells but are shifted from the crystallographic values by a quantity due to the presence of the phase term Φ_j, in $\chi(k)$ [19]. Φ_j and $|f_j(k, \pi)|$ can be transferred from a system to another, provided that the two systems are chemically similar [20,21]. Gold phase and backscattering amplitude can be obtained analysing the EXAFS spectrum of Au bulk, since in this case the crystallographic distances are known (fig. 2).

In order to obtain information on the mean coordination numbers and on the Debye–Wallerfactors one must back-Fourier transform, one by one, the contributions to $\chi(k)$ due to the different coordination shells [22,23].

5. Results and discussion

By Fourier transforming EXAFS spectra of our samples we obtained the values reported in table 2. As can be seen, also in figs. 3 and 4, as the cluster size decreases the interatomic distances of the first (R_{I}) and second (R_{II}) coordination shells decrease. This clearly shows the presence of a contraction in the interatomic distances that amounts to 2.5% for the first coordination shell and to 2.9% for the second one. Values obtained for the second coordination shells are in good agreement with that reported by Boswell [7], relative to some Au clusters having the same mean size as ours.

We interpreted this decrease in neighbour distances with cluster size as due to the compressive force exerted by the surface tension of the small gold particles. On the other hand, as predicted [24], our data show a linear dependence versus $1/D$ (fig. 5). In fact, for a liquid drop model, the contraction ΔR due to surface tension (f) is given by

$$\Delta R = -\tfrac{4}{3} K R_{\mathrm{b}} f / D,$$

Table 2
Values of the first (R_I) and second (R_{II}) coordination shell distances, contraction percentage ($\Delta R/R$) and ratio of R_{II} and R_I

D (Å)	R_I (Å)	$\frac{\Delta R}{R}$	R_{II} (Å)	$\frac{\Delta R}{R}$	$\frac{R_{II}}{R_I}$
Bulk	2.88	–	4.07	–	1.41
42.5	2.86	0.7	4.03	1.0	1.41
30.0	2.85	1.0	4.03	1.0	1.41
24.0	2.85	1.0	4.02	1.2	1.41
20.0	2.83	1.7	4.01	1.5	1.42
15.0	2.82	2.1	3.99	2.0	1.42
11.0	2.81	2.4	3.95	2.9	1.41

where K is the bulk compressibility, R_b is the metal bulk distance and D is the cluster mean diameter. We evaluated from fig. 5 the effective value of f, using for K the value of 5.99×10^{-13} cm^2/dyn and we obtained 3464 ± 415 dyn/cm which is in good agreement with the value $3660(\pm 30\%)$ dyn/cm reported in ref. [25].

Since we obtained, from EXAFS data, the values of R_I and R_{II} we used them in order to obtain information on the crystallographic structure of these

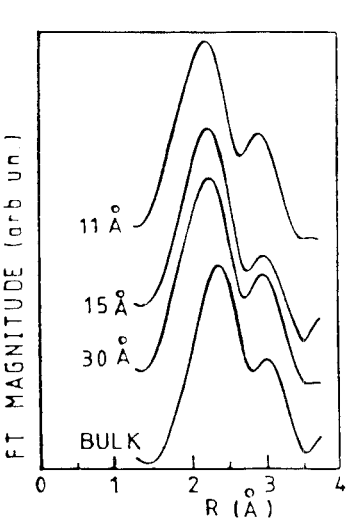

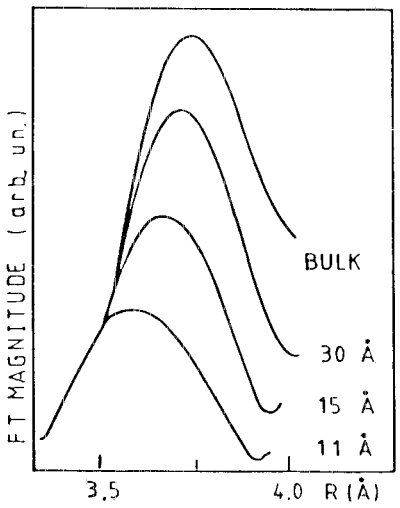

Fig. 3. Fourier transform of some films and bulk EXAFS spectra relative to the first coordination shell. The transformations are in the k range 3–11 Å^{-1} using a gaussian window and a k^1 weight.

Fig. 4. Fourier transform of some films and bulk EXAFS spectra relative to the second coordination shell using the same conditions of fig. 3.

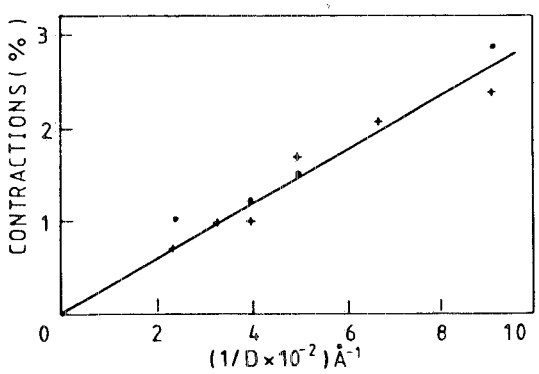

Fig. 5. Plot of the first (+) and second (●) neighbour distances contraction percentage versus the inverse of cluster mean diameter. The straight line drawn is a mean square linear fit of the data.

metal clusters. The ratio between R_{II} and R_I gives for all samples the value 1.41 (table 2) which is exactly what is expected from an fcc structure. In order to exclude further on the possible presence of changes from fcc to icosahedra structure we fitted EXAFS data relative to the first coordination shell. In the icosahedra in fact the first fcc shell is splitted in two shells, centered at distances R_1 and R_2 related by

$$R_1 = 1.05R_2.$$

We obtained that there is no presence of these two crystallographic distances.

For the first coordination shells we determined also the cluster mean coordination numbers and the Debye–Waller factors.

The experimental behaviour of the mean coordination numbers reported by Mason [1] for gold on carbon versus coverage, matches extremely well with our EXAFS results. The agreement observed [26], demonstrates that mylar, like carbon, is a weakly interacting substrate for metal clusters and states that as

Table 3
Coordination numbers (N) and Debye–Waller factors (σ^2) at RT and LNT; bulk σ^2 at LNT has been assumed equal to 1.7×10^{-3} Å^2 according to ref. [26]

D (Å)	N (±10%)	σ^2_{300K} (Å^2) (±20%)	σ^2_{77K} (Å^2) (±20%)
Bulk	12.0	4.9×10^{-3}	1.7×10^{-3}
42.5	11.0	6.7×10^{-3}	2.4×10^{-3}
30.0	10.6	7.0×10^{-3}	2.6×10^{-3}
24.0	10.0	8.6×10^{-3}	4.2×10^{-3}
20.0	9.6	10.7×10^{-3}	5.5×10^{-3}
15.0	9.4	10.0×10^{-3}	–

the cluster size decreases even the mean coordination number decreases (table 3).

EXAFS Debye–Waller factors evaluated at RT and LNT are reported in table 3. It can be seen that as the cluster size decreases the Debye–Waller factor increases. These factors at LNT can be roughly assumed as given by statical disorder contributions only. The increase in statical disorder shows that clusters grow in an fcc structure less ordered than the bulk. On the other hand, the increase of $\sigma^2_{300\ \mathrm{K}}$ in comparison to $\sigma^2_{77\ \mathrm{K}}$ has a dynamical origin: as the cluster size decreases there is an increase of surface atoms that have an higher mobility with respect to bulk ones.

6. Conclusions

The main results reported in this work can be summarized as a real presence of contractions in Au small metal particles, but no changes from fcc structure to icosahedra one are revealed down to clusters of 11 Å. The behaviour of these contractions is well understood using a macroscopic liquid drop model. The increased surface to volume ratio determines a decrease of the cluster mean coordination number and an increase of statical and dynamical contributions to disorder as the cluster size decreases.

References

[1] M.G. Mason, Phys. Rev. B27 (1983) 748.
[2] H. Roulet, J.M. Mariot, G. Dufour and C.F. Hague, J. Phys. F10 (1980) 1025.
[3] G. Apai, J. Hamilton, J. Stohr and A. Thompson, Phys. Rev. Letters 43 (1979) 165.
[4] J.L. Dormann, Rev. Phys. Appl. 16 (1981) 275.
[5] J.P. Borel, Surface Sci. 106 (1981) 1.
[6] J. Sinfelt, Rev. Mod. Phys. 51 (1979) 569.
[7] F.W.C. Boswell, Proc. Phys. Soc. (London) 64A (1951) 465.
[8] C. Berry, Phys. Rev. 88 (1952) 596.
[9] H.J. Wasserman and S.J. Vermaak, Surface Sci. 22 (1970) 164.
[10] C.L. Briant and J.J. Burton, Surface Sci. 51 (1975) 345.
[11] M.B. Gordon, F. Cyrot-lackmann and M.C. Desjonquères, Surface Sci. 106 (1980) 159.
[12] B. Moraweck and A.J. Renouprez, Surface Sci. 106 (1981) 35.
[13] P.A. Lee, P.H. Citrin, P. Eisenberger and B.M. Kincaid, Rev. Mod. Phys. 53 (1981) 769.
[14] J.P. Marton and J.R. Lemon, Phys. Rev. B4 (1971) 271.
[15] S. Normann, T. Andersson, L.G. Granqvist and O. Hunderi, Phys. Rev. B18 (1978) 674.
[16] R. Barbini et al., Riv. Nuovo Cimento 4 (1981).
[17] E. Burattini et al., Nucl. Instr. Methods 208 (1983) 91.
[18] S. Mobilio, F. Comin and L. Incoccia, LNF internal report 82/19(NT) (1982).
[19] D.E. Sayers, E.A. Stern and F.W. Lytle, Phys. Rev. Letters 35 (1975) 584.
[20] P.H. Citrin, P. Eisenberger and B.M. Kincaid, Phys. Rev. Letters 36 (1976) 1346.
[21] E.A. Stern, B.A. Bunker and S.M. Heal, Phys. Rev. B21 (1980) 1346.

[22] G. Martens, P. Rabe, N. Schwenter and A. Werner, Phys. Rev. B17 (1978) 1481.
[23] P. Rabe, Japan. J. Appl. Phys. 17 (1978) 22.
[24] C.W. Mays, J.S. Vermaak and D. Kuhlmann-Wilsdorf, Surface Sci. 12 (1968) 134.
[25] D. Schroeer et al., Phys. Rev. B2 (1970) 4414.
[26] A. Balerna et al., Phys. Rev. B31 (1985).